Linear, Super-Linear and Combined Fourier Heat Kernel Convergence Estimates for Schwarz Waveform Relaxation

Martin J. Gander and Véronique Martin

1 Introduction

We are interested in solving the heat equation $\partial_t u - \tilde{\nu}\partial^2_{xx} u = f$ on $(-L, L) \times (0, T)$, with an initial condition and with Dirichlet boundary conditions. We will use a Schwarz Waveform Relaxation (SWR) method and want to study the convergence of this algorithm. More precisely our goal is to understand the influence of T and L on the convergence. We therefore study the equation on an adimentionalized domain

$$\begin{aligned} \mathcal{L}u &:= \frac{\partial u}{\partial t} - \nu \frac{\partial u}{\partial x^2} = f \quad \text{on } (-1,1) \times (0,1), \\ u(-1,\cdot) &= g_{-1}, \\ u(1,\cdot) &= g_1, \\ u(\cdot,0) &= u_0, \end{aligned} \tag{1}$$

where $\nu = \frac{\tilde{\nu} T}{L^2} > 0$. Then it suffices to study the influence of ν on the convergence speed of the algorithm.

We will consider the SWR algorithm with Dirichlet boundary conditions ($\delta > 0$ is the overlap)

$$\begin{array}{llll} \mathcal{L}u_1^k = f & \text{on } (-1,\delta) \times (0,1), & \mathcal{L}u_2^k = f & \text{on } (0,1) \times (0,1), \\ u_1^k(\delta,\cdot) = u_2^{k-1}(\delta,\cdot) & \text{on } (0,1), & u_2^k(0,\cdot) = u_1^k(0,\cdot) & \text{on } (0,1), \\ u_1^k(\cdot,0) = u_0 & \text{on } (-1,\delta), & u_2^k(\cdot,0) = u_0 & \text{on } (0,1), \\ u_1^k(-1,\cdot) = g_{-1} & \text{on } (0,1), & u_2^k(1,\cdot) = g_1 & \text{on } (0,1). \end{array} \tag{2}$$

Martin J. Gander
Section de Mathématiques, Université de Genève, Suisse, e-mail: martin.gander@unige.ch

Véronique Martin
UMR CNRS 7352, Université de Picardie Jules Verne, Amiens, France, e-mail: veronique.martin@u-picardie.fr

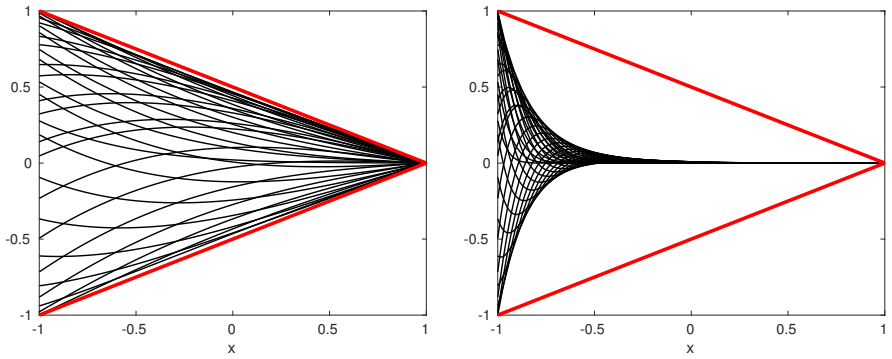

Fig. 1 Solution (in black) at several time steps of the heat equation (1) when $g_{-1}(t) = \sin(3\pi t)$, $g_1(t) = 0$ for $\nu = 10$ (left) or $\nu = 0.1$ (right). In red the bound given by Lemma 1.

The error $e_j^k := u - u_j^k$, $j = 1, 2$ satisfies by linearity again the same algorithm (2) but with homogeneous data, i.e. $f = 0$, $u_0 = 0$, $g_{-1} = g_1 = 0$.

In Sections 2 and 3 we recall convergence results proved using the maximum principle and we give numerical illustrations to understand the domain of validity of each convergence bound. Then we explain in Section 4 how the Fourier transform is usually used to measure the convergence speed of the algorithm and we discuss this strategy when it is applied to a stationary or to an unstationary equation. We end in Section 5 with numerical results to summarize the different regimes of convergence depending on the value of L and T (or equivalently on the value of ν).

2 Linear bound due to the maximum principle

In [4] a theorem is proved which gives a linear bound for the error corresponding to algorithm (2). It relies on

Lemma 1 *If u is solution of the heat equation* (1) *with $u_0 = 0$, $f = 0$ then*

$$\|u(x,\cdot)\|_\infty \le ((1-x)\|g_{-1}\|_\infty + (x+1)\|g_1\|_\infty)/2, \ -1 \le x \le 1,$$

where $\|g\|_\infty = \sup_{t\in[0,1]} |g(t)|$.

Note that this bound does not depend on the value of ν. If ν is large then u tends to satisfy $\partial_{xx} u \simeq 0$ and then u tends to be linear. The bound is sharp in this case. However, if ν is small the solution tends to decay rapidly away from the boundary and is close to 0 except near $x = -1$ and $x = 1$ where boundary layers appear. The bound is not sharp in this case. In Figure 1 we show examples of the solution of the heat equation in these two cases. Using Lemma 1, the following theorem is proved in [4]:

Theorem 1 *The error of algorithm* (2) *satisfies for any $k \ge 1$*

$$\|e_1^k(0,\cdot)\|_\infty \le \left(\frac{1-\delta}{1+\delta}\right)^k \|e_1^0(0,\cdot)\|_\infty.$$

We expect this bound to be sharp for small spatial domains or large time, corresponding to the case of a large value of ν.

3 Superlinear bound

In [4] a superlinear bound is proved for the error of the algorithm (2):

Theorem 2 *The error in algorithm* (2) *satisfies for any* $k \geq 1$ *the superlinear bound*

$$\|e_1^k(0,\cdot)\|_\infty \leq erfc\left(\frac{k\delta}{2\sqrt{\nu}}\right)\|e_1^0(0,\cdot)\|_\infty,$$

where $erfc(x) = \frac{2}{\sqrt{\pi}}\int_x^{+\infty} e^{-t^2}dt$ *is the complementary error function.*

The proof (see [4]) consists in comparing $e_1^k(0,\cdot)$ and $\overline{e}_1^k(0,\cdot)$ where $\overline{e}_1^k$ is defined on an infinite spatial domain by

$$\begin{cases} \mathcal{L}\overline{e}_1^k = 0 & \text{on } (-\infty,\delta)\times(0,1), \\ \overline{e}_1^k(\cdot,0) = 0 & \text{on } (-\infty,\delta), \\ \overline{e}_1^k(\delta,t) = \max\limits_{0\leq\tau\leq t}|e_2^{k-1}(\delta,\tau)| & \text{on } (0,1), \\ \lim\limits_{x\to-\infty}\overline{e}_1^k(x,t) = 0 & \text{on } (0,1). \end{cases}$$

Using the maximum principle we have

$$|e_1^k(0,t)| \leq \overline{e}_1^k(0,t) = \int_0^t \|e_2^{k-1}(\delta,\cdot)\|_{L^\infty(0,\tau)}K(\delta,t-\tau)d\tau,$$

where the last equality is obtained since in the infinite domain $(-\infty,\delta)$ the solution $\overline{e}_1^k(0,t)$ can be computed using the heat kernel $K(x,t) = \frac{x}{2\sqrt{\pi}}\frac{e^{-\frac{x^2}{4t}}}{t^{3/2}}$. The result is then obtained by induction. In Figure 2 we compare e_1^k and $\overline{e}_1^k$. We can see that for a large value of ν the superlinear bound is not sharp (due to the fact that $\overline{e}_1^k$ is computed on an infinite spatial domain) while for a small ν a boundary layer has appeared and the superlinear bound gives a sharper estimate than the linear bound.

4 Analysis using Fourier arguments

While in [4] and [5] the SWR for the heat equation were studied using arguments coming from the PDE analysis, in [6] a method is proposed to use the Fourier transform to obtain the convergence factor of a Schwarz algorithm for the stationary convection-diffusion equation, and this technique was rapidly also applied to a time dependent equation in [2], namely the heat equation.

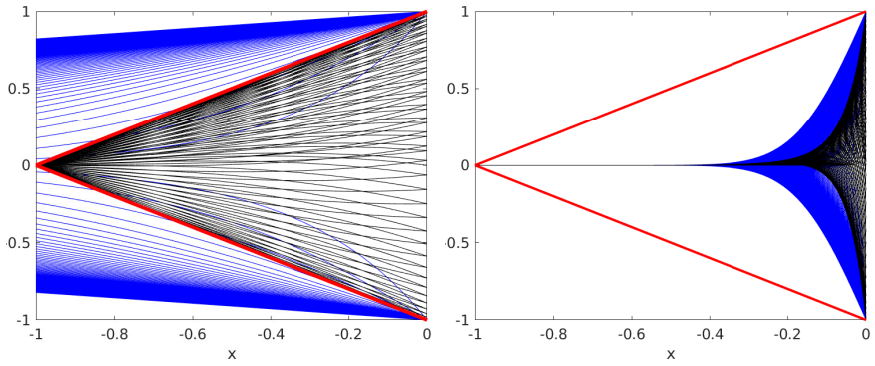

Fig. 2 Comparison of $e_1^k(\cdot,t)$ (in black) and $\overline{e}_1^k(\cdot,t)$ (in blue) for several values of t. Here $\delta = 0$ and $\nu = 10$ (left) or $\nu = 0.01$ (right). In red the bound given by Lemma 1.

In the infinite spatial domain $\mathbb{R}$ and infinite time domain $\mathbb{R}^+$, the strategy in the time dependent case consists in solving algorithm (2) for the errors in Laplace variables. If $s := \sigma + i\omega$, $\sigma, \omega \in \mathbb{R}$ let $\hat{f}(s) = \int_0^{+\infty} f(t)e^{-st}dt$, $\Re(s) \geq \alpha$ be the Laplace transform of the function $f \in L^1(\mathbb{R})$ such that $|f(t)| \leq Ce^{\alpha t}$, $C > 0$ and α constants.

We first obtain

$$\hat{e}_1^k(x,s) = \alpha^k e^{\sqrt{\frac{s}{\nu}}x} \quad \text{and} \quad \hat{e}_2^k(x,s) = \beta^k e^{-\sqrt{\frac{s}{\nu}}x}.$$

We suppose that the algorithm for the error is initialized with $e_2^0(\delta,t) = g(t)$. By induction using the Dirichlet boundary conditions we obtain

$$\hat{e}_1^k(0,s) = \rho(s)^{(2k-1)}\hat{g}(s),$$

where $\rho(s) := e^{-\sqrt{\frac{s}{\nu}}\delta}$ is the convergence factor of the algorithm.

This formula seems to say that $\rho(\sigma + i\omega)$ explains the convergence behavior of the single frequency ω. We will see in the next subsections that this is true for a stationary problem like the screened Laplace equation. However the situation is more complex for an unstationary problem like the heat equation. To understand this point, let us back-transform the previous formula to obtain

$$e_1^k(0,t) = \int_0^t g(t-\tau)K((2k-1)\frac{\delta}{\sqrt{\nu}},\tau)d\tau, \tag{3}$$

where $K(x,t) = \frac{x}{2\sqrt{\pi}}\frac{e^{-\frac{x^2}{4t}}}{t^{3/2}}$ is the heat kernel. We see that the error is expressed as a convolution between the heat kernel and g.

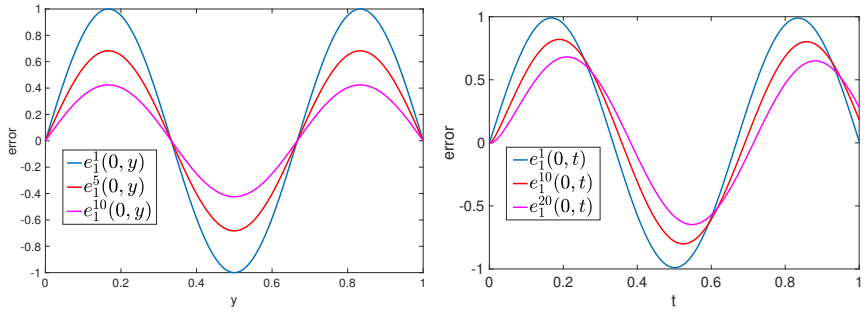

Fig. 3 On the left, errors $e_1^k(0,y)$ for the screened equation at iterations $k=1$, $k=5$ and $k=10$ when the first guess is $e_2^0(\delta,y)=\sin(3\pi y)$. On the right, errors $e_1^k(0,t)$ for the heat equation at iterations $k=1$, $k=10$ and $k=20$ when the first guess is $e_2^0(\delta,t)=\sin(3\pi t)$.

4.1 Using Fourier arguments is different for time dependent and stationary problems

To understand the difference between the stationary case and the unstationary one, we first consider the screened Laplace equation $\tilde{\mathcal{L}}u := \eta u - \triangle u = f$ in $\Omega := \mathbb{R}^2$, with $\eta > 0$. If the domain Ω is split into the two overlapping subdomains $\Omega_1 := (-\infty,\delta)\times\mathbb{R}$ and $\Omega_2 := (0,+\infty)\times\mathbb{R}$, where $\delta > 0$ is the overlap parameter, then the classical Schwarz algorithm (for the errors) solves for iteration index $k=1,\ldots$

$$\begin{array}{ll} \tilde{\mathcal{L}}e_1^k = 0 & \text{on } (-\infty,\delta)\times\mathbb{R}, \\ e_1^k(\delta,\cdot) = e_2^{k-1}(\delta,\cdot) & \text{on } \mathbb{R}, \end{array} \qquad \begin{array}{ll} \tilde{\mathcal{L}}e_2^k = 0 & \text{on } (0,+\infty)\times\mathbb{R}, \\ e_2^k(0,\cdot) = e_1^k(0,\cdot) & \text{on } \mathbb{R}. \end{array} \tag{4}$$

If the initial error is a pure sine signal on the interface, $e_2^0(\delta,y) := \sin(\lambda y)$, then the errors for each iteration $k=1,2,\ldots$ can be obtained by a direct computation to be

$$e_1^k(0,y) = e^{-(2k-1)\delta\sqrt{\eta+\lambda^2}}\sin(\lambda y) =: \tilde{\rho}(\lambda)^{2k-1}\sin(\lambda y),$$

which means that at each iteration the initial sine error is contracted by the convergence factor $\tilde{\rho}(\lambda)$. This result is consistent with the definition of the convergence factor in [1] which was obtained by a Fourier transform in the y direction with Fourier variable ω.

In Figure 3 left, we can see the errors $e_1^k(0,y)$ at iterations $k=1$, $k=5$ and $k=10$. The initial sine is contracted as the iterations grow as predicted by the previous formula. Let us see what happens for the heat equation (Figure 3, right): a sine is introduced ($e_2^0(\delta,t) := \sin(\lambda t)$) and we can see now that the sine is not just contracted anymore, it is also transported! We can use the formula (3) to understand that $e_1^k(0,t)$ is not anymore a sine function. We need therefore a more detailed analysis which is given in the next section.

4.2 Analysis for the heat equation

If the Fourier analysis were relevant for the heat equation, then introducing a pure sine frequency in the algorithm would give a pure sine frequency at any iteration $k > 0$, which is not the case as we saw in the previous subsection. A better understanding of the behavior of the pure sine frequency can be obtained from the following theorem, proved in [3].

Theorem 3 *Let $T = +\infty$ and $L = +\infty$. If the Schwarz Waveform Relaxation algorithm* (2) *is initialized with the pure sine frequency $e_2^0(\delta, t) = \sin(\lambda t)$, then the error is given by*

$$e_1^k(0,t) = |\rho(\lambda)|^{2k-1} \sin\left(\lambda t - (2k-1)\delta\sqrt{\frac{\lambda}{2\nu}}\right) + z_2\left((2k-1)\frac{\delta}{\sqrt{\nu}}, t; \lambda\right),$$

where z_2 satisfies for large frequency λ

$$z_2\left((2k-1)\frac{\delta}{\sqrt{\nu}}, t; \lambda\right) = \frac{1}{\lambda} K\left((2k-1)\frac{\delta}{\sqrt{\nu}}, t\right) + O\left(\frac{1}{\lambda^3}\right),$$

and for large iteration k

$$\left\| z_2\left((2k+1)\frac{\delta}{\sqrt{\nu}}, \cdot; \lambda\right)\right\|_{L^\infty(0,+\infty)} \sim \left(\frac{2k-1}{2k+1}\right)^2 \left\| z_2\left((2k-1)\frac{\delta}{\sqrt{\nu}}, \cdot; \lambda\right)\right\|_{L^\infty(0,+\infty)}.$$

An analogous result also holds for e_2^k.

This theorem states that if you introduce a pure sine frequency as the initial guess, then along the iterations the error becomes a sine which is contracted by ρ but which is also translated. In addition the sine is distorted by a term proportional to the heat kernel K.

5 Numerical results

In this section we illustrate the previous results with numerical experiments. An implicit scheme in time is used to discretize the heat equation. The spatial and time discretization parameters are $\Delta x = \Delta t = \frac{2}{2001}$ and the overlap is $\delta = 5\Delta x$. We will consider two values for ν so that we will obtain the different behaviors described in the previous sections.

We first consider the value $\nu = 1000$ which corresponds to a small spatial domain, or large time. The initial guess is the pure sine $e_2^0(\delta, t) = \sin(25t)$. In Figure 4 left, we show the error at $x = \delta$ as a function of t at iterations $k = 0$ and $k = 100$. We see that the sine is exactly contracted, which we can understand using Figure 4 right: ν is so large that the error is linear and the convergence is dictated by the maximum

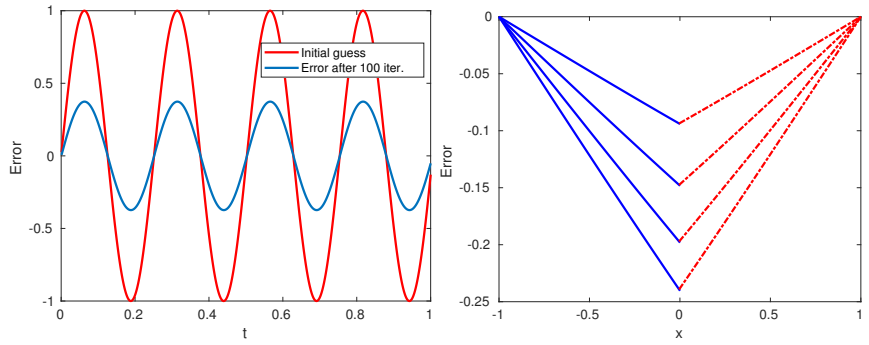

Fig. 4 $\nu = 1000$. On the left, the error $e_1^k(0,t)$ as a function of t. On the right, the error $e_1^k(x, t = 0.9965)$ as a function of x at iterations 1, 20, 50 and 100.

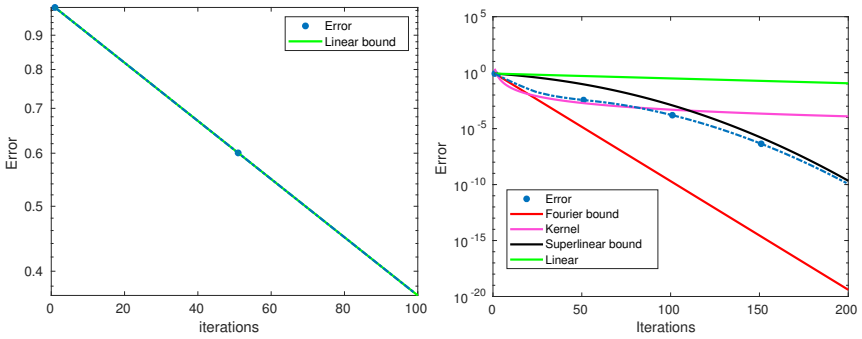

Fig. 5 Error $\|e_1^k(0,\cdot)\|_\infty$ as function of the Schwarz Waveform Relaxation iterations k. On the left $\nu = 1000$, on the right $\nu = 0.05$.

principle described in Section 2. This result is confirmed in Figure 5, left, where we show the norm of the error versus the iterations: we exactly obtain the linear bound described in Section 2.

We then consider the value $\nu = 0.05$ which corresponds to a large spatial domain, or small time interval. The initial guess is the pure sine $e_2^0(\delta,t) = \sin(50t)$.

In Figure 6 we show the solution as a function of x at $t = 0.1$. We see that now the boundary conditions at $x = \pm 1$ do not influence the solution and the behavior is not linear anymore. In Figure 7 we show the error $e_1^k(\delta,t)$ as a function of t for iterations $k = 10$, $k = 30$ and $k = 45$. We see that the initial guess $\sin(50t)$ is not only contracted, it is also translated and transformed by the heat kernel. In Figure 5 right, we show the error as a function of the iterations. The convergence is first guided by the Fourier convergence factor. For later iterations however, the heat kernel we observed in Figure 7 becomes dominant for the convergence mechanism of the Schwarz Waveform Relaxation algorithm. Then the heat kernel leaves the time domain and the superlinear regime dominates.

We have thus shown that for time dependent problems, Fourier analysis techniques can be applied to study Schwarz Waveform Relaxation algorithms, but care must be

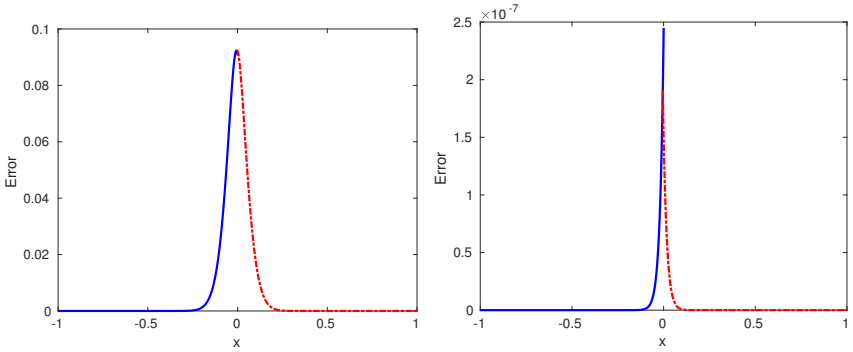

Fig. 6 $\nu = 0.05$. Error $e_1^k(x, t = 0.1)$ as a function of x at iterations 10 and 50.

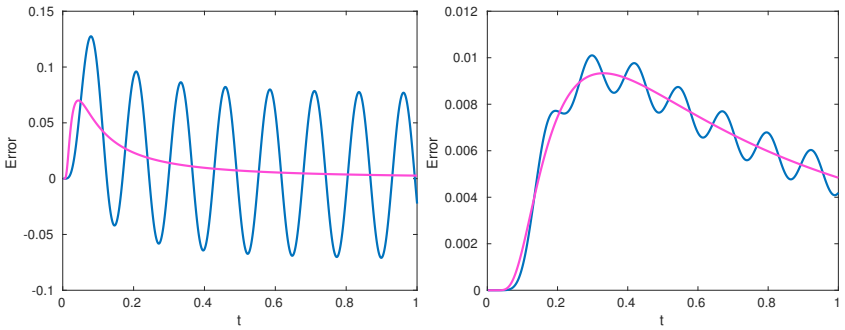

Fig. 7 $\nu = 0.05$. Error $e_1^k(0, t)$ as a function of t from left to right at iterations $k = 10$ and $k = 30$. In magenta the heat kernel term $\frac{1}{\lambda} K\left((2k-1)\frac{\delta}{\sqrt{\nu}}, t\right)$.

taken due to the evolution nature of the problem: Fourier modes initially still contract for diffusion problems away from the initial conditions as expected, but eventually heat kernel components dominate and change the convergence behavior.

References

1. Gander, M. J. Optimized schwarz methods. *SIAM Journal on Numerical Analysis* **44**(2), 699–731 (2006).
2. Gander, M. J. and Halpern, L. Méthodes de relaxation d'ondes (SWR) pour l'équation de la chaleur en dimension 1. *C. R. Math. Acad. Sci. Paris* **336**(6), 519–524 (2003).
3. Gander, M. J. and Martin, V. Why fourier mode analysis in time is different when studying schwarz waveform relaxation. *Accepted for publication in Journal of Computational Physics* (2023).
4. Gander, M. J. and Stuart, A. M. Space-time continuous analysis of waveform relaxation for the heat equation. *SIAM J. Sci. Comput.* **19**(6), 2014–2031 (1998).
5. Giladi, E. and Keller, H. B. Space-time domain decomposition for parabolic problems. *Numer. Math.* **93**(2), 279–313 (2002). URL https://doi.org/10.1007/s002110100345.
6. Japhet, C., Nataf, F., and cois Rogier, F. The optimized order 2 method: Application to convection–diffusion problems. *Future Generation Computer Systems* **18**(1), 17–30 (2001). I. High Performance Numerical Methods and Applications. II. Performance Data Mining: Automated Diagnosis, Adaption, and Optimization.